Composites Communications 17 (2020) 177–181

Contents lists available at ScienceDirect

Composites Communications

journal homepage: www.elsevier.com/locate/coco

Short Communication

In-situ synthesis of microspherical Sb@C composite anode with high tap density for lithium/sodium-ion batteries

Junjian Tian [1], Hao Yang [1], Cuimei Fu, Minglin Sun, Lina Wang [*], Tianxi Liu

State Key Laboratory for Modification of Chemical Fibers and Polymer Materials, College of Materials Science and Engineering, Innovation Center for Textile Science and Technology, Donghua University, Shanghai, 201620, China

ARTICLE INFO

Keywords:
Stibium
Microspherical anode material
Li-ion batteries
Na-ion batteries

ABSTRACT

The search for anode materials that suitable for both lithium-ion and sodium-ion batteries is one of the most top challenges in the field of rechargeable batteries. In this work, Sb@C composites are synthesized via in-situ calcination of as-prepared micro-spherical Sb_2O_3 in the presence of polyethylene glycol (PEG), which acts as a reductive agent and carbon source. The Sb@C composites with a structure of microspheres are composed of crystalline Sb nanoparticles coated by interconnected porous carbon. Such an unique structure not only provides a stable conductive matrix, but also leads to a high tap density of 1.35 g cm^{-3}. A specific capacity of 280 mAh g^{-1} can be retained at 100 mA g^{-1} after 500 cycles for lithium-ion batteries and 130 mA g^{-1} at 100 mA g^{-1} after 100 cycles for sodium-ion batteries.

1. Introduction

Graphite material, which displays a flat charge–discharge platform and a superior cycling stability, has been occupied a dominant position among anode materials for lithium-ion batteries (LIBs) [1,2]. However, the relatively low theoretical capacity of graphite (372 mAh g^{-1}) limits the energy density of LIBs. And security issues may arise in the case of overcharge due to the discharge platform of graphite (0.1–0.2 V vs. Li/Li^+) is very close to the potential for deposition of Li. Sodium-ion batteries (SIBs) are now actively revisited as an alternative for LIBs because of the natural abundance, low cost and environmental benignity of Na resources [3]. The ionic radius of the Na^+ is 55% larger than that of the Li^+, which makes graphite can not be used as a host material to accommodate Na^+. Over the last few decades, stibium (Sb) has been received extensive attention due to a higher theoretical capacity (660 mAh g^{-1}) with a flat discharge platform (~0.85 V vs. Li/Li^+) [4–7]. Besides, Sb can be used not only in LIBs but also meet the requirements of SIBs to form the Li_3Sb or Na_3Sb alloy [5–8]. However, the severe volume change of Sb-based anode materials leads to the rapid capacity decay during cycling [9–11].

So far, much efforts have been devoted to overcome these issues. The introduction of a carbon matrix to make carbon coated Sb (Sb@C) composites is a plausible strategy. Carbon can improve the conductivity as well as prevent the pulverization and agglomeration of the composites [12–14]. Through rational design of the structure can effectively improve the cyclic performance. For example, Sb@C coaxial nanotube was successfully synthesized by Liu et al. via a carbon-coating method followed by a thermal reduction [14]. Fan et al. synthesized Sb@C microrods by reducing the as-prepared Sb_2O_3 microrods with C_2H_2, which showed a lithium storage capacity of 478.8 mAh g^{-1} at a current density of 100 mA g^{-1} after 100 cycles [6]. Wu et al. synthesized Sb@C nanofibers through a single-nozzle electrospinning technique and subsequent calcination, which delivered a large reversible capacity of 337 mAh g^{-1} at a current rate of 5 C after 400 cycles [7]. Kim et al. and Hou et al. prepared Sb hollow nanospheres by utilizing SiO_2 or Ni nanosphere as templates [15,16]. The porous structure was introduced acting as buffer layers to retard volume changes and shorten lithium diffusion distance. Although the significant advantage of the battery materials in nanoscale, a low tap density usually gives rise to a low energy density. Therefore, the applications of nanosized battery material are still limited.

Herein, microsphere-like Sb@C composites were synthesized by in-situ reducing the as-prepared Sb_2O_3 microspheres with the aid of hydrogen and carbon as the reducing agents, which are generated from pyrolysis of polyethylene glycol (PEG). Meanwhile, the nontoxic and low-cost PEG also acts as a carbon source. The as-prepared

* Corresponding author.
E-mail address: linawang@dhu.edu.cn (L. Wang).
[1] Junjian Tian and Hao Yang contributed equally.

https://doi.org/10.1016/j.coco.2019.12.005
Received 10 September 2019; Received in revised form 25 November 2019; Accepted 10 December 2019
Available online 12 December 2019

microspherical Sb@C particles were composed of uniform nanosized particles that coated with a carbon layer. Such an unique structure guarantees a high tap density (1.35 g cm^{-3}) and a smooth electronic/ionic transfer channels. Therefore, at a current density of 100 mA g^{-1}, a specific capacity of 280 mAh g^{-1} after 500 cycles for LIBs and 130 mAh g^{-1} after 100 cycles for SIBs is achieved, respectively.

2. Experimental section

2.1. Preparation of Sb_2O_3 microspherical precursor

In the synthesis, 4 mmol of $SbCl_3$ was dissolved in 40 mL of absolute ethanol and stirred for 5–10 min after magnetic stirring to obtain a colorless homogeneous solution. At the same time, 27 mL 1 M NaOH solution in a constant pressure separatory funnel was added dropwise to the solution under a magnetic stirring for 1–2 h. The solution was transferred into a Teflon-lined autoclave and kept at 150 °C for 24 h. The resulting products were collected by centrifugation and washed with distilled water and absolute ethanol, and finally dried under vacuum at 80 °C for 12 h.

2.2. Preparation of microspherical Sb@C composite

Microspherical Sb@C Composite was prepared by calcining the as-prepared Sb_2O_3 microspheres mixed with the polyethylene glycol (PEG). The dried Sb_2O_3 precursor was calcined in an electric furnace at 500 °C under continuous argon gas flow for 6–10 h at the heating rate of 5 °C min^{-1}. After cooling to room temperature, the obtained product was collected for further characterization.

2.3. Material characterization

The X-ray diffraction (XRD, D/max-2500VB+/PC, Rigalcu) patterns of the products were measured by a Cu-Kα radiation at a scan rate of 4° min^{-1}. Raman spectra were detected by a Raman Spectrometer (inVia-Reflex, Renishaw). The carbon content of Sb@C composite is approximately 38.26 wt%, which was measured by a Vario EL-III elemental analyzer. The morphology of the powder samples was evaluated by field-emission scanning electron microscopy (FE-SEM, S-4800, HITACHI) and high-resolution transmission electron microscopy (HR-TEM, JEOL JEM-2100F). The specific surface area was calculated with the multi-point Brunauer-Emmett-Teller (BET) method.

2.4. Electrochemical measurements

The anode electrode was composed of the active material, carbon black and polyvinylidene difluoride (PVdF) in a weight ratio of 80:10:10. A black viscous slurry consisting of the mixture dispersed in N-methyl-2-pyrrolidone (NMP) was cast onto a copper foil and dried in a vacuum at 150 °C for 12 h. The active material loading is 1.35 mg cm^{-2}. The electrochemical performance was measured using CR2025 coin-type cells. Li metal and a Celgard separator (25 mm thick) were used as the counter electrode and separator in Li-ion batteries. The electrolyte is 1.0 M $LiPF_6$ in ethylene carbonate (EC)/diethyl carbonate (DMC) (1:1, by V/V) solution. Na metal and a glassy fiber paper (Whatman, GF/C) were used as the counter electrode and separator in Na-ion batteries. The electrolyte is 1.0 M $NaClO_4$ in ethylene carbonate (EC)/diethyl carbonate (DMC) (1:1, by V/V) solution. The cells were assembled in an Ar-filled glove box (Mikrouna Universal). The galvanostatic cycling measurements were under a voltage range of 0.01–2.5 V using Neware Battery Measurement System (Neware, China). Cyclic voltammogramsats (CV) with a scan rate of 0.1 mV s^{-1} between 0.01 and 2.0 V and electrochemical impedance spectra (EIS) with an AC perturbation signal of 5.0 mV in the frequency range of 100 kHz–100 mHz were conducted on a CHI660C electrochemical workstation (Shanghai Chenhua, China).

3. Results and discussion

As illustrated in Fig. 1a, the microsphere-like Sb@C composite was synthesized by a precipitation reaction and followed by a heat treatment in inert atmosphere. Firstly, microspherical Sb_2O_3 precursor was synthesized via a solvothermal reaction ($2SbCl_3 + 6NaOH \rightarrow Sb_2O_3 + 6NaCl + 3H_2O$). Then, the Sb_2O_3 was reduced to Sb by hydrogen and carbon that generated from the pyrolysis of PEG, producing a strong reductive atmosphere. At the same time, the carbon layers were coated onto the Sb particles to form Sb@C composites. Fig. 1b shows XRD patterns of the Sb_2O_3 precursor and the final Sb@C product. The XRD peaks are indexed to the orthorhombic antimonous oxide Sb_2O_3 (JCPDS#43-1071) and the hexagonal Sb phase (JCPDS#35-0732), respectively. Fig. 1c shows the Raman spectrum of the Sb@C composite. Two peaks locate at 1357 and 1605 cm^{-1} are attributed to the characteristic D and G bands, respectively. D band is linked with the vibrations of the crystal border and G band represents the perfect sp^2 vibrations of graphitic crystal. The intensity ratio of D to G band is 0.86, reflecting the relatively high degree of ordering in the carbon material [17,18].

The morphological features of the Sb_2O_3 precursor and Sb@C composite are revealed by SEM. Microspheres of Sb_2O_3 precursor with an average diameter ca. 20 μm can be seen in Fig. 2a and b. These microspheres are composed of nanoparticles with an average size of ca. 200 nm (Fig. 2c). The spherical structure generally can be well kept after the calcining process with PEG (Fig. 2d). Nevertheless, slight cracks can be observed on some of the Sb@C microspheres, and the surface becomes rougher (Fig. 2e) and porous (Fig. 2f). Owing to gas release from the pyrolysis of PEG upon the heat treatment, continuous porous carbon matrix is readily formed in the Sb@C particles. Such an unique structure guarantees a high tap density of 1.35 g cm^{-3}. The ground particles were taken for TEM observations. The TEM image shown in Fig. S1a clearly indicates the homogeneous distribution of Sb nanograins (black dots) in the carbon matrix (grey color), which can enhance conductivity and structural stability [19–23]. The high-resolution TEM image (Fig. S1b) shows the average size of the Sb nanograins is 5–10 nm. The clear lattice fringes with an interplanar spacing of 0.311 nm correspond to the (012) plane of the Sb crystal structure (JCPDS#35-0732). To further explore the porous structure and specific surface area of the Sb@C composite, N_2 adsorption-desorption isotherms and the pore size distribution analysis were carried out. The N_2 adsorption-desorption plots in Fig. 3a suggest a dramatically increased surface area of Sb@C (177 m^2 g^{-1}) compared with Sb_2O_3 (7.7 m^2 g^{-1}). In addition, the pore size distribution analysis suggests that the micropores smaller than 2 nm and mesopores of 4 nm of Sb@C are increased significantly compared with that of Sb_2O_3 (Fig. 3b). The hierarchical construction would prevent the pulverization/aggregation of the ultrafine Sb nanoparticles and relieve the lattice strain at the particle interface upon lithiation/delithiation processes. Moreover, a high internal surface area enables the electrolyte to kinetically access the majority of Sb located in the carbon network quickly and prompt fast charge, which are vital for superior Li^+/Na^+ storage performance.

The Li^+ storage behavior of as-prepared Sb@C composite was firstly investigated with a Li-metal counter/reference electrode. The CV curves at a scan rate of 0.1 mV s^{-1} in the range of 0.01–2.5 V demonstrate a weak reduction peak occurs at 0.86 V and a subsequent sharp peak beyond 0.5 V (Fig. 4a). The sharp peak is composed of two overlapped peaks cantered at 0.78 and 0.7 V respectively (inset in Fig. 4a). The three reduction peaks can be assigned to the step-wise alloying reactions of Sb with Li to form Li_xSb and finally to Li_3Sb. During the reverse positive scan, one overlapped sharp and one weak oxidation peak emerge at 1.16 and 1.39 V, corresponding to the dealloying reaction of Li_3Sb [24,25]. In following cycles, the peak potential positions are well-overlapped without obvious shift although the peak currents are slightly decreased. There is no any current peak can be observed in voltage range below 0.5 V, indicating any Li-intercalated graphite as charge carrier can be ruled out [26]. The overall electrochemical reaction of the Sb@C

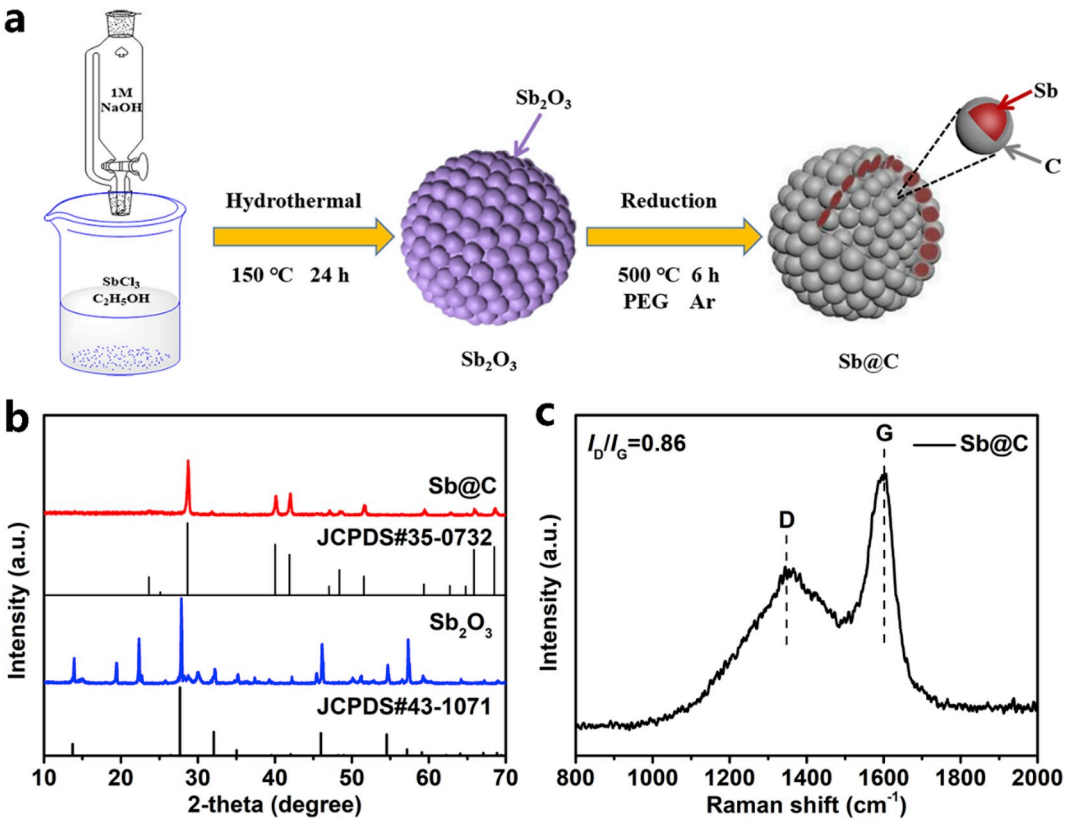

Fig. 1. (a) Illustration of the formation process of the Sb@C composite, (b) XRD pattern and (c) Raman spectrum of the Sb@C composite.

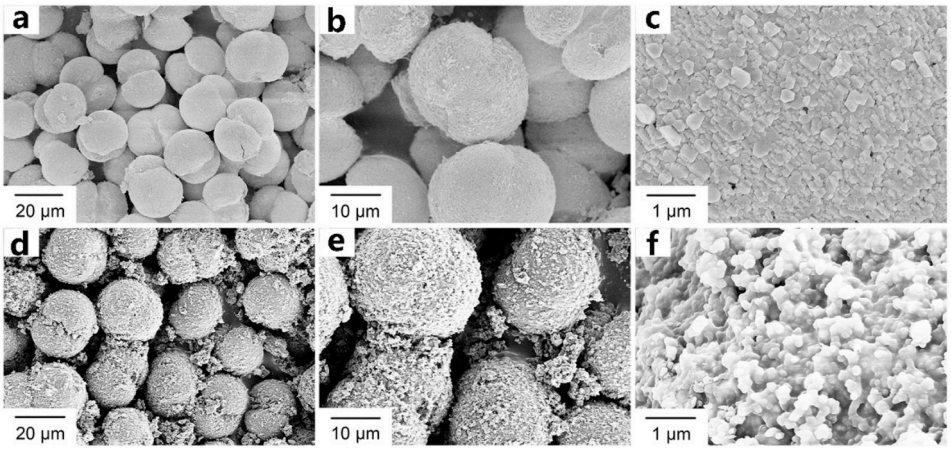

Fig. 2. SEM images of (a–c) the Sb_2O_3 precursor and (d–f) the Sb@C composite.

with Li can be expressed as eqns (1) and (2).

$$Sb + 3Li^+ + 3e^- \rightarrow Li_3Sb \quad (1)$$

$$Li_3Sb - 3Li^+ - 3e^- \rightarrow Sb \quad (2)$$

Fig. 4b shows the charge and discharge profiles of the Sb@C anode composite in the initial three cycles between 0.01 and 2.5 V at a constant current density of 100 mA g^{-1}. The discharge and charge of the first cycle are 1135.1 mAh g^{-1} and 721.6 mAh g^{-1} respectively, and the corresponding coulombic efficiency (CE) is 63.5%. The low initial CE denotes an irreversible decomposition of the electrolyte for the formation of solid-electrolyte interface [27]. From the second cycle, the CE is basically stable at 100%. However, capacity fading is observed in the initial cycles, which should be resulted from the somewhat volumetric change of the electrodes upon repeated delithiation/lithiation processes. A relatively stabilized capacity can be obtained after the initial cycles and the reversible capacity maintains at 280 mAh g^{-1} after 500 cycles (Fig. 4c). As various current densities, the Sb@C composite exhibits a reversible capacity of 626.4, 525.3, 472.4, 427.6, and 336.8 mAh g^{-1} at 100, 200, 300, 400 and 500 mA g^{-1} respectively. The decent cycle performance and rate capability indicate the potential of the microsphere-like Sb@C composite as a candidate anode material. EIS measurements of Sb@C composite before and after cycling were carried out, as shown in Fig. S2. The pristine electrode exhibits a charge transfer resistance (R_{ct}) of 466 Ω. The R_{ct} is reduced to a much lower value of 341 Ω after cycling at 100 mA g^{-1}, suggesting the smooth reaction kinetics.

The Sb@C with a Na metal counter/reference electrode in SIBs

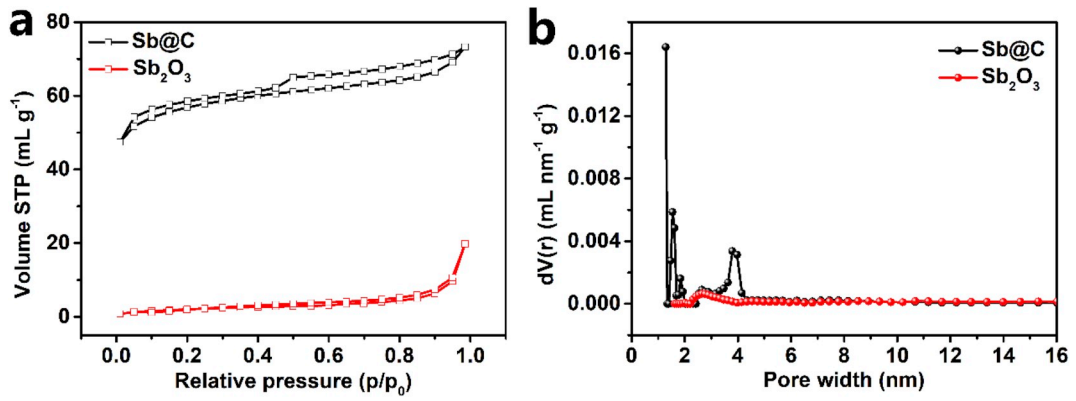

Fig. 3. (a) N_2 adsorption-desorption isotherms and (b) pore size distributions of the Sb_2O_3 and the Sb@C composite.

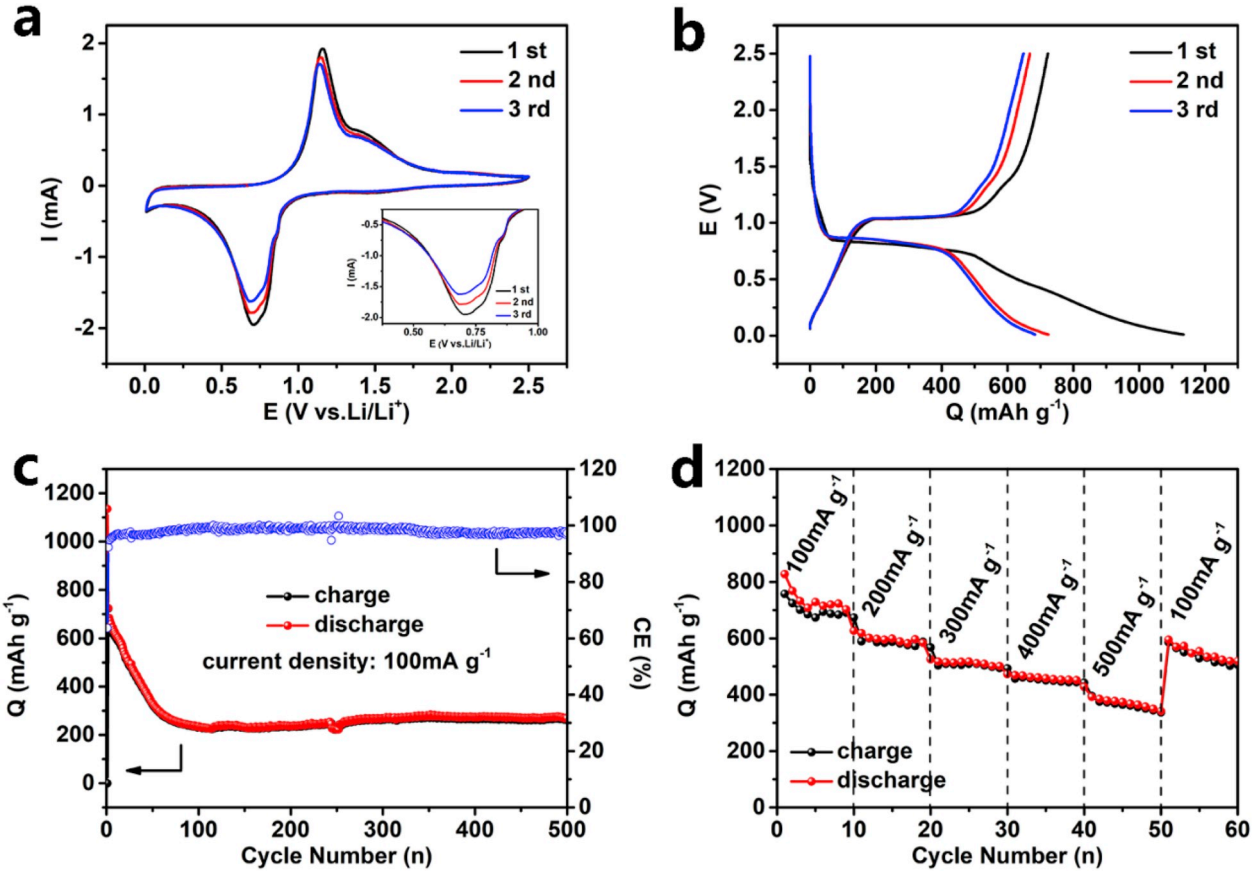

Fig. 4. The electrochemical performance of Sb@C composite in Li-ion batteries. (a) CV curves in the initial three cycles within 0.01–2.5 V, (b) Discharge/charge voltage profiles at 100 mA g^{-1}, (c) Cycling performance and (d) Rate capability.

demonstrates a similar electrochemical behavior. The reduction peaks in CV curves (Fig. S3a) centered at 0.72 and 0.45 V can be attributed to the sodiation of Sb to form Na_3Sb, while the inverse oxidation peak at 0.8 and 1 V indicates the desodiation of Na_3Sb [28,29], suggesting the reversibility of the alloying reaction. The galvanostatic discharge/charge profiles shows a similar feature with their LIB counterpart (Fig. S3b). The cyclic performance in Fig. S3c shows the Sb@C electrode maintains a capacity of 130 mAh g^{-1} at 100 mA g^{-1} after 100 cycles. The CE of is as high as 98.4% for over 100 cycles, indicating a good reaction reversibility. The Sb@C composite electrode displays a reversible capacity of 160, 100.7, 80 and 68.5 mAh g^{-1} at 100, 200, 300, 400 and 500 mA g^{-1}, respectively (Fig. S3d). When the current decrease to 100 mA g^{-1}, the capacity recovers to 161.5 mAh g^{-1}. Notably, due to the larger ionic radius of Na^+ (1.02 Å) than Li^+ (0.76 Å) and the higher equivalent weight of Na than Li, the impact on the structure of host materials becomes more serious [30]. Therefore, the Sb@C composite shows a stronger tolerance for the rapid alloying/dealloying reaction with Li^+ than Na^+.

4. Conclusions

The work presents a facile strategy to fabricate the porous electrode material with high tap density. The microspherical Sb@C composite was successfully prepared by calcining the mixture of the as-prepared microspherical Sb_2O_3 precursors with PEG under inert atmosphere. The Sb@C composite demonstrates good Li^+/Na^+ storage and cyclic

properties, which is attributed to the continuous carbon matrix and the unique porous spherical structures. Carbon matrix as a protective layer can effectively buffer the volume changes of Sb nanocrystals during the repeated insertion/extraction processes and prompt fast the charge transport. The Sb@C composite anode exhibits a stable reversible capacity of 265 mA h g^{-1} at 100 mA g^{-1} after 500 cycles and a high rate performance of 336.8 mAh g^{-1} at 500 mA g^{-1} for LIBs. It also delivers a reversible capacity of 130 mA g^{-1} at 100 mA g^{-1} after 100 cycles for NIBs.

Author contributions

Lina Wang and Tianxi Liu conceived the work. Lina Wang, Junjian Tian and Hao Yang co-wrote the manuscript. Junjian Tian performed the experiments and analyzed the data. Hao Yang participated in data analysis. Cuimei Fu and Minglin Sun assisted with electrochemical measurements.

Declaration of competing interest

We declare that we have no competing financial interests. The work described has not been published previously, and it is not under consideration for publication elsewhere. Its publication is approved by all authors and tacitly by the responsible authorities where the work was carried out. If accepted, it will not be published elsewhere in the same form, in English or in any other language, without the written consent of the publisher.

Acknowledgements

The authors acknowledge funding support from the Natural Science Foundation of Shanghai (17ZR1446400), the Fundamental Research Funds for the Central Universities (2232018D3-02), the National Natural Science Foundation of China (21603030 and 51433001), the Program of Shanghai Academic Research Leader (17XD1400100), and the Shanghai Scientific and Technological Innovation Project (18JC1410600).

Appendix A. Supplementary data

Supplementary data to this article can be found online at https://doi.org/10.1016/j.coco.2019.12.005.

References

[1] D. Pogue, Building a better battery, Sci. Am. 316 (2017) 26.
[2] B.-h. Ahn, S.-M. Lee, Preparation and characterization of spherical carbon composite for use as anode material for lithium ion batteries, Bull. Korean Chem. Soc. 31 (2010) 1331–1335.
[3] H. Yu, Y. Ren, D. Xiao, S. Guo, Y. Zhu, Y. Qian, L. Gu, H. Zhou, An ultrastable anode for long-life room-temperature sodium-ion batteries, Angew. Chem. Int. Ed. 53 (2014) 8963–8969.
[4] J. Song, P. Yan, L. Luo, X. Qi, X. Rong, J. Zheng, B. Xiao, S. Feng, C. Wang, Y.-S. Hu, Y. Lin, V. Sprenkle, X. Li, Yolk-shell structured Sb@C anodes for high energy Na-ion batteries, Nano Energy 40 (2017) 504–511.
[5] N. Zhang, Y. Liu, Y. Lu, X. Han, F. Cheng, J. Chen, Spherical nano-Sb@C composite as a high-rate and ultra-stable anode material for sodium-ion batteries, Nano Res. 8 (2015) 3384–3393.
[6] L. Fan, J. Zhang, J. Cui, Y. Zhu, J. Liang, L. Wang, Y. Qian, Electrochemical performance of rod-like Sb-C composite as anodes for Li-ion and Na-ion batteries, J. Mater. Chem. 3 (2015) 3276–3280.
[7] L. Wu, X. Hu, J. Qian, F. Pei, F. Wu, R. Mao, X. Ai, H. Yang, Y. Cao, Sb-C nanofibers with long cycle life as an anode material for high-performance sodium-ion batteries, Energy Environ. Sci. 7 (2014) 323–328.
[8] J. Qian, Y. Chen, L. Wu, Y. Cao, X. Ai, H. Yang, High capacity Na-storage and superior cyclability of nanocomposite Sb/C anode for Na-ion batteries, Chem. Commun. 48 (2012) 7070–7072.
[9] X. Zhou, Y. Zhong, M. Yang, M. Hu, J. Wei, Z. Zhou, Sb nanoparticles decorated N-rich carbon nanosheets as anode materials for sodium ion batteries with superior rate capability and long cycling stability, Chem. Commun. 50 (2014) 12888–12891.
[10] K. Ramakrishnan, C. Nithya, B.K. Purushothaman, N. Kumar, S. Gopukumar, Sb_2O_4@rGO nanocomposite anode for high performance sodium-ion batteries, ACS Sustain. Chem. Eng. 5 (2017) 5090–5098.
[11] L. Xiao, Y. Cao, J. Xiao, W. Wang, L. Kovarik, Z. Nie, J. Liu, High capacity, reversible alloying reactions in SnSb/C nanocomposites for Na-ion battery applications, Chem. Commun. 48 (2012) 3321–3323.
[12] Z. Yi, Q. Han, P. Zan, Y. Wu, Y. Cheng, L. Wang, Sb nanoparticles encapsulated into porous carbon matrixes for high-performance lithium-ion battery anodes, J. Power Sources 331 (2016) 16–21.
[13] S. Chen, P. Chen, M. Wu, D. Pan, Y. Wang, Graphene supported Sn-Sb@carbon core-shell particles as a superior anode for lithium ion batteries, Electrochem. Commun. 12 (2010) 1302–1306.
[14] Z. Liu, X.-Y. Yu, X. Lou, U. Paik, Sb@C coaxial nanotubes as a superior long-life and high-rate anode for sodium ion batteries, Energy Environ. Sci. 9 (2016) 2314–2318.
[15] H. Hou, M. Jing, Y. Yang, Y. Zhu, L. Fang, W. Song, C. Pan, X. Yang, X. Ji, Sodium/Lithium storage behavior of antimony hollow nanospheres for rechargeable batteries, ACS Appl. Mater. Interfaces 6 (2014) 16189–16196.
[16] H. Kim, J. Cho, Template synthesis of high-performance hollow Sb particles as a lithium battery anode material, Chem. Mater. 20 (2008) 1679–1681.
[17] Y. Yan, Z. Ma, H. Lin, K. Rui, Q. Zhang, Q. Wang, M. Du, D. Li, Y. Zhang, J. Zhu, W. Huang, Hydrogel self-templated synthesis of $Na_3V_2(PO_4)_3$@C@CNT porous network as ultrastable cathode for sodium-ion batteries, Compos. Commun. 13 (2019) 97–102.
[18] C. Portet, G. Yushin, Y. Gogotsi, Electrochemical performance of carbon onions, nanodiamonds, carbon black and multiwalled nanotubes in electrical double layer capacitors, Carbon 45 (2007) 2511–2518.
[19] Y. He, L. Huang, X. Li, Y. Xiao, G.-L. Xu, J.-T. Li, S.-G. Sun, Facile synthesis of hollow Cu_2Sb@C core-shell nanoparticles as a superior anode material for lithium ion batteries, J. Mater. Chem. 21 (2011) 18517–18519.
[20] L. Wu, H. Lu, L. Xiao, X. Ai, H. Yang, Y. Cao, Electrochemical properties and morphological evolution of pitaya-like Sb@C microspheres as high-performance anode for sodium ion batteries, J. Mater. Chem. 3 (2015) 5708–5713.
[21] G. Jung, Y. Lee, Y. Mun, H. Kim, J. Hur, T. Kim, K. Suh, J. Kim, D. Lee, W. Choi, I. Kim, Sb-$AlC_{0.75}$-C composite anodes for high-performance sodium-ion batteries, J. Power Sources 340 (2017) 393–400.
[22] J. Kong, H. Wei, D. Xia, P. Yu, High-performance Sb_2S_3/Sb anode materials for Li-ion batteries, Mater. Lett. 179 (2016) 114–117.
[23] J. Liu, L. Yu, C. Wu, Y. Wen, K. Yin, F.-K. Chiang, R. Hu, J. Liu, L. Sun, L. Gu, J. Maier, Y. Yu, M. Zhu, New nanoconfined galvanic replacement synthesis of hollow Sb@C yolk-shell spheres constituting a stable anode for high-rate Li/Na-ion batteries, Nano Lett. 17 (2017) 2034–2042.
[24] J. Hassoun, G. Derrien, S. Panero, B. Scrosati, The role of the morphology in the response of Sb-C nanocomposite electrodes in lithium cells, J. Power Sources 183 (2008) 339–343.
[25] T. Yang, H. Wang, J. Xu, L. Wang, W.-C. Song, Y. Maocd, J. Ma, Preparation of a Sb/Cu_2Sb/C composite as an anode material for lithium-ion batteries, RSC Adv. 6 (2016) 78959–78962.
[26] X. Wang, Y. Qian, L. Wang, H. Yang, H. Li, Y. Zhao, T. Liu, Sulfurized polyacrylonitrile cathodes with high compatibility in both ether and carbonate electrolytes for ultrastable lithium-sulfur batteries, Adv. Funct. Mater. (2019) 1902929.
[27] L. Wu, X. Hu, J. Qian, F. Pei, F. Wu, R. Mao, X. Ai, H. Yang, Y. Cao, Sb-C nanofibers with long cycle life as an anode material for high-performance sodium-ion batteries, Energy Environ. Sci. 7 (2014) 323–328.
[28] A. Darwiche, C. Marino, M.T. Sougrati, B. Fraisse, L. Stievano, L. Monconduit, Better cycling performances of bulk Sb in Na-ion batteries compared to Li-ion systems: an unexpected electrochemical mechanism, J. Am. Chem. Soc. 134 (2012) 20805–20811.
[29] Y. Zhu, X. Han, Y. Xu, Y. Liu, S. Zheng, K. Xu, L. Hu, C. Wang, Electrospun Sb/C fibers for a stable and fast sodium-ion battery anode, ACS Nano 7 (2013) 6378–6386.
[30] W. Shen, C. Wang, Q. Xu, H. Liu, Y. Wang, Nitrogen-doping-induced defects of a carbon coating layer facilitate Na-storage in electrode materials, Adv. Energy Mater. 5 (2015) 1400982.